

Scattering of ${}^6\text{He}$ at energies around the Coulomb barrier

A.M. Sánchez-Benítez[†], D. Escrig^{||}, M.A.G. Álvarez[‡], M.V. Andrés[‡], C. Angulo⁺, M.J.G. Borge^{||}, J. Cabrera⁺, S. Cherubini[§], J.M. Espino[‡], P. Figuera[§], M. Freer[‡], J.E. García-Ramos[†], J. Gómez-Camacho[‡], M. Gulino[§], O.R. Kakuee[¶], I. Martel[†], C. Metelco[‡], A.M. Moro[‡], J. Rahighi[¶], K. Rusek[†], D. Smirnov^{*}, O. Tengblad^{||}, P. Van Duppen^{*}, V. Ziman[‡]

[†]Departamento de Física Aplicada, Universidad de Huelva, E-21071 Huelva, Spain

[‡]Departamento de Física Atómica, Molecular y Nuclear, Universidad de Sevilla, E-41080 Sevilla, Spain

^{||} Instituto de Estructura de la Materia, CSIC, E-28006 Madrid, Spain

[¶]Van der Graaff Laboratory, Nuclear Research Centre, AEOI, PO Box 14155-1339, Tehran, Iran

⁺ Centre de Recherches du Cyclotron, Université catholique de Louvain, B-1348 Louvain-la-Neuve, Belgium

^{*} Instituut voor Kern-en Stralingsfysica, University of Leuven, B-3001 Leuven, Belgium

[‡] School of Physics and Space Research, University of Birmingham, B15 2TT Birmingham, England

[§]INFN Laboratori Nazionali del Sud and Sezione di Catania, I-95123 Catania, Italy

E-mail: angel.sanchez@dfaie.uhu.es

Abstract. We have measured elastic cross sections of the scattering of ${}^6\text{He}$ at $E_{Lab} = 14, 16, 17, 18, 22$ MeV on ${}^{208}\text{Pb}$ in the angular ranges of $20^\circ - 64^\circ$ and $135^\circ - 170^\circ$. A significant amount of ${}^4\text{He}$ events is found at energies well below the Coulomb barrier, that becomes dominant above it. Optical Model calculations have been performed including a dynamic polarization potential. Very large imaginary diffuseness parameter is needed in order to describe the experimental distributions.

PACS numbers: 01.30.Cc; 13.75.-n; 24.10.Ht; 25.10.+s; 25.60.Dz; 25.60.Gc; 25.60.Bx; 21.10.Gv; 27.20.+n

Submitted to: *J. Phys. G: Nucl. Phys.*

1. Introduction

The interest in studying the elastic scattering of ^6He arises from its weakly bound nature, which significantly affects the dynamics of the collision. This nucleus is known to have a well developed 3-body structure consisting on an alpha particle and two valence neutrons weakly bound by less than 1 MeV [1, 2]. Coupling to the states from the continuum may play an important role in the dynamics of the reaction process by means of long range reaction mechanisms. In particular, we are interested in continuum states coupled with the ground state of ^6He by the dipole component of the Coulomb field of the target. That is what Coulomb dipole polarizability accounts for, and it has been found that it gives rise to a significant reduction of the elastic cross sections for other systems [3, 4, 5].

In this paper we report on measurements of elastic scattering and alpha production cross sections of $^6\text{He}+^{208}\text{Pb}$ at Coulomb barrier energies. Due to the high Z value of target and the relatively low scattering energy, we expect important effects from the Coulomb dipole coupling.

2. Experiment

The experiment was performed at the Centre de Recherches du Cyclotron at Louvain-la-Neuve, Belgium [6]. The bombarding energies of the secondary ^6He beam were 14, 16, 17, 18 and 22 MeV, with a current intensity on target of about 5×10^6 pps (10^6 pps for the 22 MeV beam). Accelerated ^6He ions were scattered on a self supported target with the following isotopic composition: ^{208}Pb 87(2)%, ^{207}Pb 1.20(2)%, ^{206}Pb 11.4(2)%. A target of 0.950 mg/cm^2 thickness was used for each energy except for 22 MeV, where beam intensity was lower and a thickness of 2.080 mg/cm^2 was chosen. Elastic scattering cross sections of a 12 MeV ^4He beam from ^{208}Pb was also measured to normalize data and to cancel systematic errors in the $^6\text{He}+^{208}\text{Pb}$ elastic cross sections.

Two 5 mm collimators were used to provide good beam definition and to reduce frame scattering events. The outgoing particles were detected by three arrays of detectors, LEDA (used in standard and LAMP configurations) and DINEX. Figure 3 shows a schematic lay-out of the experimental set up.

LEDA silicon strip detectors (SSD) are described in [7]. DINEX detector array (see figure 1) consists of four 90° circular silicon telescopes, of thickness $40\mu\text{m}$ (front) and $500\mu\text{m}$ (back). The front detector is a single sided SSD detector, a so called CD-type strip detector [8]. DINEX detector array was able to achieve a good identification of ^4He and ^6He events with an adequate angular resolution (see figure 2). LEDA, LAMP and DINEX detector arrays cover three different angular ranges (see figure 3): LEDA $5^\circ - 12^\circ$ with an angular resolution of 0.5° , LAMP $20^\circ - 64^\circ$ with an angular resolution of 3° , and DINEX $135^\circ - 170^\circ$ with an angular resolution of 5° . The solid angle covered by LEDA+LAMP+DINEX arrays was 33% of 4π . Corrections for beam alignment and efficiency of the electronic chain were also evaluated and included in the final analysis. As an example the elastic cross section divided by the Rutherford cross section obtained

at 18 and 22 MeV are shown in figure 4, and the alpha production cross section at the energy of 22 MeV is shown in figure 5.

The LAMP region includes the onset of Rutherford scattering regime at lower angles, providing us the needed reference experimental points for a global normalization. Therefore the analysis of the data from LEDA region is redundant, whereas implies additional nontrivial corrections due to the high rate of detected particles.

3. Analysis

We carried out an optical model (OM) analysis of the experimental data using the code ECIS [9]. In the calculations the effects of the dipole couplings to the states in the continuum were included by means of a dynamic dipole polarization potential (DDPP) [10]. Its Coulomb part was calculated explicitly from the theoretically predicted B(E1) energy distribution [11]. In the analysis we used a Coulomb radius of $R_C = 9.29$ fm. For the nuclear potential we have chosen Woods-Saxon radial form factors for both real and imaginary parts with a radius $R_r = R_i = 10.07$ fm [12]. We made a fit to the 22 MeV distribution by means of four-parameter search. The depths and diffusenesses of the nuclear potential were varied in the search, with the starting values taken from [12]. The energy of 22 MeV is above the Coulomb barrier so the calculations are expected to be sensitive to the parameters of the nuclear potential.

The value of the imaginary diffuseness obtained at 22 MeV ($a_i=2(1)$ fm) fits well the data also at lower energies. This very large value suggests the presence of the strong nuclear component of the DDPP. The Coulomb component was explicitly included in the calculations. This result is in accordance with previous experimental works [12, 13, 14].

Solid curves in figure 4 are OM calculations using $a_i=2.21$ fm. Only the depths were varied in the search for the energy of 18 MeV. In order to see the effect of the large imaginary diffuseness and the sensitivity of the result, OM calculations were also performed with a fixed and more standard value for $a_i=0.819$ fm. This value was used in [15] for the scattering of ^6Li on ^{208}Pb . The result of this calculation is shown in figure 4 (dotted curves). The large imaginary diffuseness obtained for ^6He dumps oscillations in the region of the Coulomb rainbow.

Preliminary coupled channels calculations were performed for the energy of 22 MeV, assuming a simple di-neutron model of ^6He . The couplings with the states from the continuum were included by means of continuum - discretized coupled - channels (CDCC) technique. The OM calculations with $a_i=2.21$ fm (solid curve) and CDCC calculations (dashed curve) fit the experimental data equally well, although at intermediate scattering angles they lead to quite different results. This calls for new experimental data in this angular range.

In order to tackle the process of neutron transfer to the target, another approach was adopted assuming that the detected alpha particles at backward angles were produced via the transfer of a fully correlated di-neutron cluster to either the target bound states or continuum states, the latter accounting for the breakup contribution. Both processes

were treated using the prior form of the DWBA amplitude. The calculated angular distributions of the alpha particles are compared with the experimental data in figure 5.

4. Summary and outlook

We have investigated the elastic scattering of ^6He on ^{208}Pb at bombarding energies $E_{\text{Lab}} = 14, 16, 17, 18, 22$ MeV in a wide range of angles. A significant amount of ^4He events is found at energies well below the Coulomb barrier, that becomes dominant above it.

Optical model calculations including a dynamic dipole polarization potential can reproduce properly the data, provided that a very large imaginary diffuseness is used. Thus, Coulomb dipole polarizability accounts only for part of the absorption from elastic channel. Data at 22 MeV can be equally well described by the CDCC calculations. The transfer of 2n to the target and direct break-up were included simultaneously in a different approach, achieving partially to reproduce alpha production cross section.

New scattering data would be needed to fully understand the mechanism of ^6He interaction with ^{208}Pb in the vicinity of the Coulomb barrier.

Acknowledgments

The authors would like to thank the staff at the CYCLONE RIB facility at the Cyclotron Research Centre in Louvain-la-Neuve, Belgium, for providing us with an intense and good quality radioactive beam. This work has been partially supported by the Spanish Dirección General de Investigación, Ciencia y Tecnología under projects number FPA2000-1592-C03-02, FPA2002-04181-C04-02/04, the Belgian program P5/07 on interuniversity attraction poles of the Belgian-state Federal Services for Scientific, Technical and Cultural Affairs, and the European Community-Access to Research Infrastructure action of the Improving Human Potential Programme, contract N^o HPRI-CT-1999-00110. A. M. S. B. acknowledges a research grant from the Spanish MCyT.

References

- [1] Tanihata I, 1996 *J. Phys. G: Nucl. Part. Phys.* **22** 157-8
- [2] Hansen P G and Jonson B, 1987 *Europhysics Letters* **4** 409-14
- [3] Andrés M V, Gómez-Camacho J and Nagarajan M A, 1995 *Nucl. Phys.* **583A** 817-20
- [4] Moro A M and Gómez-Camacho J, 1999 *Nucl. Phys.* **648A** 141-56
- [5] Martel I, Gómez-Camacho J, Rusek K *et al .*, 1998 *Nucl. Phys.* **641A** 188-202
- [6] Vervier J, 1997 *Nucl. Phys.* **616A** 97c-106c
- [7] Davinson T, Brandfield-Smith W, Cherubini S, *et al .*, 2000 *Nucl. Instrum. Methods* **454A** 350-8
- [8] Ostrowski A N, Cherubini S, Davinson T, *et al .*, 2002 *Nucl. Instrum. Methods* **480A** 448-55
- [9] Raynal J, 1981 *Phys. Rev.* **23C** 2571-85
- [10] Andrés M V, Gómez-Camacho J and Nagarajan M A, 1994 *Nucl. Phys.* **579A** 273-84

- [11] Thompson I J, Danilin B V, Efros V D, *et al.* , 2000 *Phys. Rev.* **61C** 24318
- [12] Kakuee O R, Rahighi J, Sánchez-Benítez A M, *et al.* , 2003 *Nucl. Phys.* **728A** 339-49
- [13] Aguilera E F, Kolata J J, Nunes FM, *et al.* , 2000 *Phys. Rev. Lett.* **84** 5058-61
- [14] Aguilera E F, Kolata J J, Becchetti F D, *et al.* , 2001 *Phys. Rev.* **63C** 061603-6
- [15] Keeley N , Bennett S J, Clarke N M, *et al.* , 1994 *Nucl. Phys.* **571A** 326-36

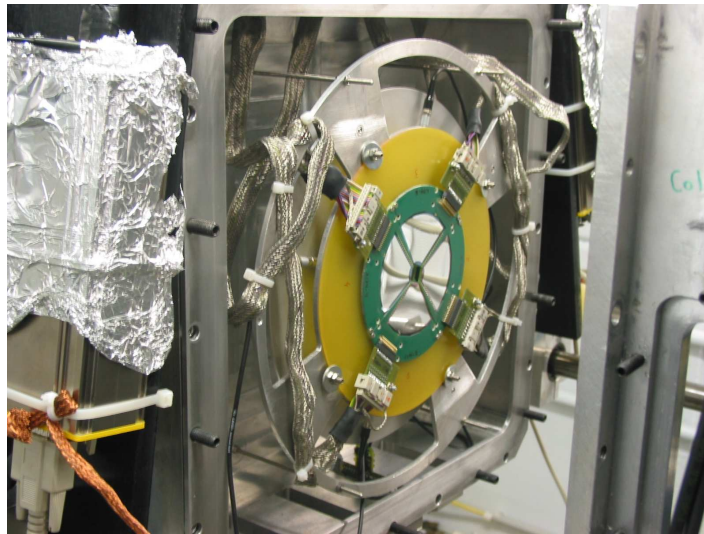


Figure 1. DINEX detector array.

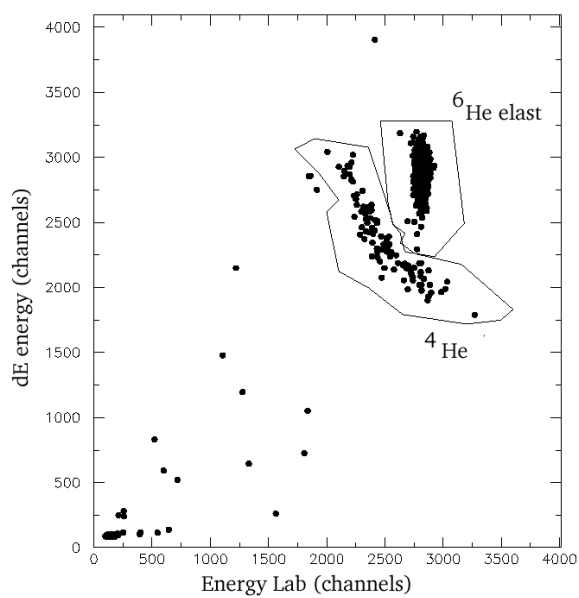


Figure 2. Mass spectrum at $E = 14\text{ MeV}$, $\theta_{lab} = 161^\circ$ obtained with DINEX detector array.

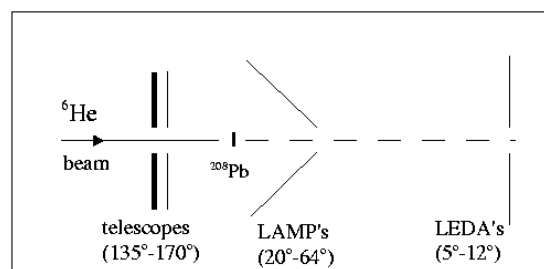


Figure 3. Sketch of the experimental set-up.

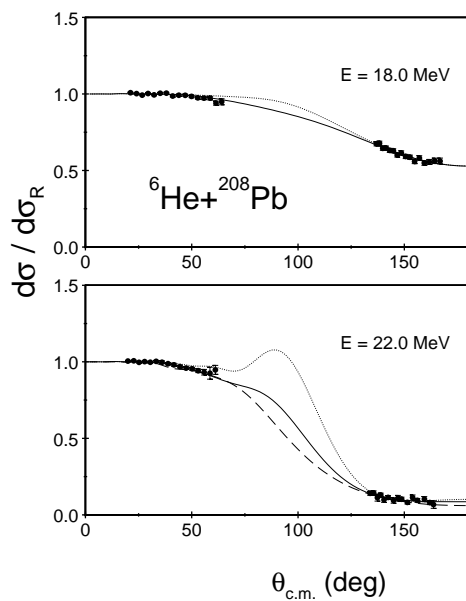


Figure 4. Angular distributions of elastic cross section divided by the Rutherford cross section compared with OM and CDCC calculations.

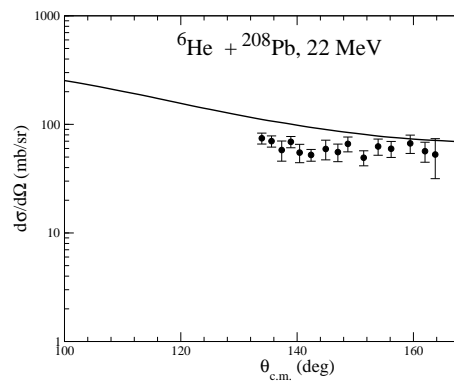


Figure 5. Angular distribution of alpha production cross section compared with DWBA calculation.